



## Molecular Crystals and Liquid Crystals

Publication details, including instructions for authors and subscription information:

<http://www.tandfonline.com/loi/gmcl20>

### CHARACTERISTIC IMPROVEMENTS OF ORGANIC ELECTROLUMINESCENT DEVICES BY ASSISTED DOUBLE-CARRIER INJECTIONS

Jae-Hoon Park<sup>a</sup>, Yun-Hee Kwak<sup>a</sup>, Yong-Soo Lee<sup>a</sup>,  
Jong Sun Choi<sup>a</sup>, Sung-Taek Lim<sup>b</sup> & Dong-Myung Shin<sup>b</sup>

<sup>a</sup> Department of Electrical, Information, and Control Engineering, Hongik University, 72-1 Sangsu-dong, Mapo-gu, Seoul, Korea

<sup>b</sup> Department of Chemical Engineering, Hongik University, 72-1 Sangsu-dong, Mapo-gu, Seoul, Korea

Version of record first published: 15 Jul 2010

To cite this article: Jae-Hoon Park, Yun-Hee Kwak, Yong-Soo Lee, Jong Sun Choi, Sung-Taek Lim & Dong-Myung Shin (2003): CHARACTERISTIC IMPROVEMENTS OF ORGANIC ELECTROLUMINESCENT DEVICES BY ASSISTED DOUBLE-CARRIER INJECTIONS, Molecular Crystals and Liquid Crystals, 405:1, 105-112

To link to this article: <http://dx.doi.org/10.1080/15421400390262498>

PLEASE SCROLL DOWN FOR ARTICLE

Full terms and conditions of use: <http://www.tandfonline.com/page/terms-and-conditions>

This article may be used for research, teaching, and private study purposes. Any substantial or systematic reproduction, redistribution, reselling, loan, sub-licensing, systematic supply, or distribution in any form to anyone is expressly forbidden.

The publisher does not give any warranty express or implied or make any representation that the contents will be complete or accurate or up to date. The accuracy of any instructions, formulae, and drug doses should be independently verified with primary sources. The publisher shall not be liable for any loss, actions, claims, proceedings, demand, or costs or damages whatsoever or howsoever caused arising directly or indirectly in connection with or arising out of the use of this material.

## CHARACTERISTIC IMPROVEMENTS OF ORGANIC ELECTROLUMINESCENT DEVICES BY ASSISTED DOUBLE-CARRIER INJECTIONS

*Jae-Hoon Park, Yun-Hee Kwak, Yong-Soo Lee,  
and Jong Sun Choi*

*Department of Electrical, Information, and Control  
Engineering, Hongik University, 72-1 Sangsu-dong,  
Mapo-gu, Seoul, Korea*

*Sung-Taek Lim and Dong-Myung Shin*  
*Department of Chemical Engineering, Hongik University,  
72-1 Sangsu-dong, Mapo-gu, Seoul, Korea*

*Energy barriers exist at the interfaces between electrodes and organic layers, and interrupt carrier injections. Deteriorated carrier injections result in increasing the driving voltage and lowering the efficiency of organic electroluminescent devices (OLEDs). The assisted double-carrier injections into organic layers can be achieved by lowering these energy barriers. Thin  $\alpha$ -septithiophene ( $\alpha$ -7T) layer was inserted for buffer layer and composite cathode composed of CsF and Al was formed in order to enhance hole and electron injections, respectively. The orientations of  $\alpha$ -7T molecules were adjusted by rubbing method and the mass ratio of CsF was varied between 1 and 10 wt%. Upon the investigations, it is believed that the mass ratio of CsF, 3 wt% and the horizontal orientation of  $\alpha$ -7T molecules are the optimized conditions for the performance of OLEDs. The characteristics of OLEDs with these structures are improved due to the increased carrier injections and the balanced carrier densities in the emission region.*

**Keywords:**  $\alpha$ -septithiophene; alkaline metal; buffer layer; composite cathode; OLEDs

### INTRODUCTION

Since Tang and Van Slyke have developed organic electroluminescent devices (OLEDs) [1], many efforts have been made to improve the device efficiency [2–4]. Device efficiency is highly dependent on carrier injecting processes at electrode and organic interfaces. And carrier recombination

This work was supported by the Korea Research Foundation (KRF-2001-005-D22001).

efficiency is an important factor affecting the emission efficiency [5]. Enhanced carrier injections and transport to the emission region do not ensure the improved device efficiency. OLEDs efficiency strongly depends on balanced carrier injections from electrodes and efficient recombination of carriers at emission region [6]. Organic conducting layer, inserted between anode and organic layer, and low work function cathode are commonly used in the modified OLED structure, for hole and electron injection, respectively.

In this work, we demonstrate that organic electroluminescent (EL) device efficiency can be improved by assisted double-carrier injections. Thin  $\alpha$ -7T layer was inserted for buffer layer. CsF and Al were co-evaporated for composite cathode. The assisted double-carrier injections could be achieved with these structures and its effects on the device characteristics will be discussed.

## EXPERIMENTAL DETAILS

Devices were fabricated on ITO-patterned glass substrates. The ITO film had a sheet resistance of less than  $20\Omega/\square$  and was about 100-nm-thick. And ITO-patterned substrates were cleaned in an ultrasonic bath of acetone, followed by isopropyl alcohol, and then D. I. water. They were dried in nitrogen gas flow and conveyed to a vacuum oven to be heated up to  $180^\circ\text{C}$  for 20 min in order to eliminate the residual solution. The molecular structures of the organic materials and the schematics of OLEDs used in this study are shown in Figure 1. Organic layers were deposited in the following sequence: An  $\alpha$ -7T layer was deposited onto ITO as a buffer layer; then, 50-nm-thick TPD [N, N'-diphenyl-N, N'-bis(3-methylphenyl)-1, 1'-biphenyl-4-4'-diamine] and 50-nm-thick  $\text{Alq}_3$  [tris(8-hydroxyquinoline) aluminum] were deposited as the hole-transporting and the electron-transporting layers, respectively, under a base pressure of  $1.6 \times 10^{-6}$  Torr. At last, 100-nm-thick cathode was formed under the same pressure.

The rubbing process for the horizontal orientation of  $\alpha$ -7T molecules is shown in Figure 2 [7]. In depositing the Al-CsF composite contact, the mass ratio of alkaline metal was varied from 1 to 10 wt%. The effective cell area, which is defined with the overlap region between the anode and the cathode, was  $0.09\text{cm}^2$ . Thicknesses were confirmed using ellipsometry (Plasmos, SD-2100) and  $\alpha$ -step profilometer (Tenkor, 200). UV/vis absorption was measured using HP 8452A unit. A positive bias was applied to the ITO with respect to the cathode. The current-voltage measurements were performed using Keithley 238 source-measurement unit. All measurements were carried out under an ambient atmosphere and at room temperature.

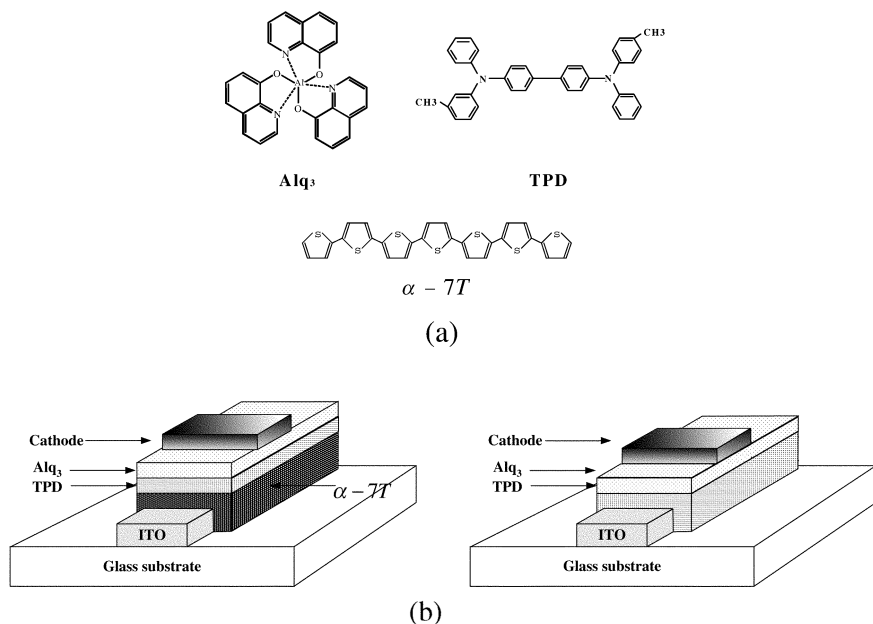


**FIGURE 1** (a) Molecular structures of organic materials and (b) schematics of OLEDs.

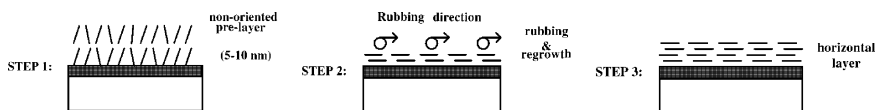


**FIGURE 2** Schematic description of the rubbing process.

## RESULTS AND DISCUSSIONS

### 1. Characteristics of OLEDs With $\alpha$ -7T Buer Layer

The absorption spectra of  $\alpha$ -7T layers with different molecular orientations under polarized lights are shown in Figure 3. For the horizontal molecular orientation to the substrate, the rubbing method was carried out as shown in Figure 2. In the absorption spectra of  $\alpha$ -7T film (50 nm) with rubbing-induced molecular orientation, the absorption is strong when the light is parallel to the rubbing direction while the absorption becomes very weak when the light is perpendicular to the rubbing direction. The dichroic ratio,  $R = A_{\parallel}/A_{\perp}$ , is 4.2 at 438 nm, where  $A_{\parallel}$  and  $A_{\perp}$  are the absorbances parallel

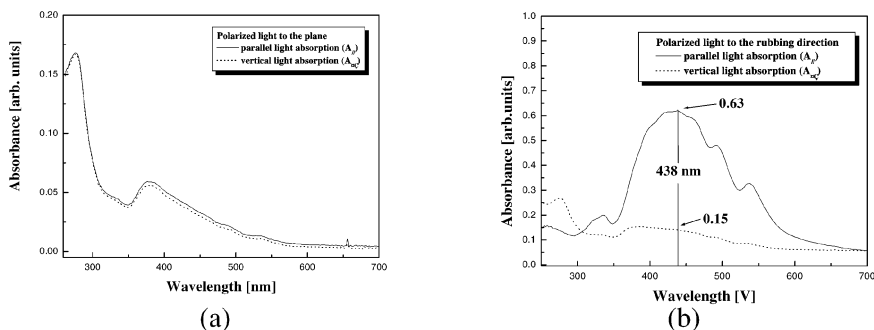


**FIGURE 3** UV/vis spectra of (a) the un-rubbed  $\alpha$ -7T layer and (b) the rubbed  $\alpha$ -7T layer.

and perpendicular to the substrate, respectively. Spectra present a broad-band peak at 438 nm with satellites at 488 and 534 nm. These structures are assigned to the fundamental  $\pi$ - $\pi^*$  transition of the isolated molecule and its vibronic replicas [7]. The fundamental  $\pi$ - $\pi^*$  band peak at 438 nm becomes highly dichroic. Meanwhile, dichroism is not observed in the absorption spectra for an un-rubbed  $\alpha$ -7T layer. Only broad-band peak at 380 nm can be observed. These results show that the orientations of the rubbed  $\alpha$ -7T molecules are parallel to each other and horizontal to the substrate.

In the previous paper, the effects of the  $\alpha$ -7T molecular orientations on the electrical properties of the device were reported [8]. Horizontal alignment of  $\alpha$ -7T molecules results in a conductivity increase of more than one order of magnitude (from  $1.2 \times 10^{-6}$  S/cm for the  $\alpha$ -7T layer to  $1.7 \times 10^{-5}$  S/cm for the rubbed  $\alpha$ -7T layer). These results are attributed to enhanced hole-transport along the highest occupied molecular orbital (HOMO) column running through the horizontal film [9]. The dependence of the OLED performances on the  $\alpha$ -7T layer thickness was also investigated. The current density ( $J$ )-voltage ( $V$ ) characteristics are shown in Figure 4. The inclusion of buffer layers has only a modest effect on the efficiency as long as these layers are sufficiently thin (below 20 nm) [10]. Therefore, it is considered that the horizontally oriented  $\alpha$ -7T layer (20 nm) is suitable for enhancing the device characteristics from Figure 4.

## 2. Characteristics of OLEDs With Composite Cathode

The current density-voltage characteristics of the devices with the composite cathodes are shown in Figure 5. The mass ratio of CsF was varied from 1 to 10 wt%. The devices with the composite cathodes show superior performance to the device with Al cathode. Low operation voltages were obtained, which is attributed to the efficient electron injections.

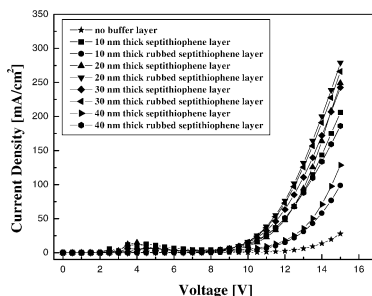


**FIGURE 4**  $J$ - $V$  characteristics of OLEDs according to the different thicknesses of  $\alpha$ -7T layer.

CsF molecules are decomposed when contact with Al atoms. The energy level of organic layer is adjusted due to the diffused cesium ions into the organic layer. The electron from fluorine is transferred back to the cesium atom and an extra charge gets transferred to the organic layer. As a result, the contact formed at the organic/cathode interface becomes ohmic [11]. It is reported that Cs is evaporated onto  $\text{Alq}_3$  and diffused uniformly into  $\text{Alq}_3$  so that the Fermi level moves toward the lowest unoccupied molecular orbital (LUMO) level of  $\text{Alq}_3$  [12]. Therefore, efficient electron injections can be achieved by lowered energy barrier. It is considered that the cathode composed of Al-CsF (3 wt%) is suitable for improving the device performances from Figure 5.

### 3. Characteristics of OLEDs With the Assisted Double Carrier Injections

From the above-mentioned results, horizontally oriented  $\alpha$ -7T layer (20 nm), as a buffer layer, was interposed between ITO and TPD layer. And composite cathode of Al-CsF (3 wt%) was formed. The energy levels of

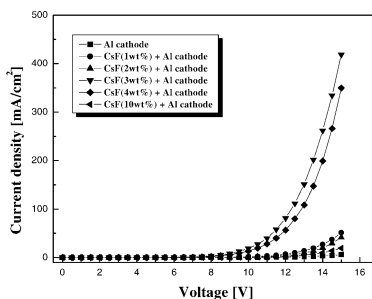


**FIGURE 5**  $J$ - $V$  characteristics of OLEDs with composite cathode according to the mass ratios of alkaline metal.

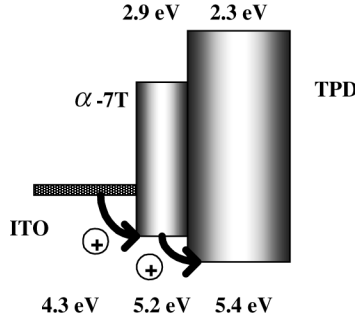


**FIGURE 6** Hole injection process via  $\alpha$ -7T buffer layer.

$\alpha$ -7T layer were measured using cyclic volt-current measurements. Possible hole injection process is illustrated in Figure 6. It seems that hole injections become easier via stair-like energy barrier. In electron injections, barrier heights from Fowler-Nordheim tunneling equation were calculated as 0.22 eV for the device with composite cathode and 0.26 eV for the device with Al cathode. This lowered barrier height allows electrons to inject into TPD with easy. As a result, the inserted  $\alpha$ -7T buffer layer and the composite cathode enhanced hole and electron injections, respectively. Therefore, the assisted double-carrier injections could be obtained. Fowler-Nordheim tunneling equation is as follows. Used parameters have general meanings.

$$J = \frac{A^* T^2}{\phi_B} \left( \frac{qF}{\alpha k T} \right)^2 \exp \left[ -\frac{2\alpha \phi_B^{3/2}}{3qF} \right]$$

The current density-voltage and the luminance ( $L$ )-voltage ( $V$ ) characteristics of the fabricated devices are shown in Figure 7. Device by

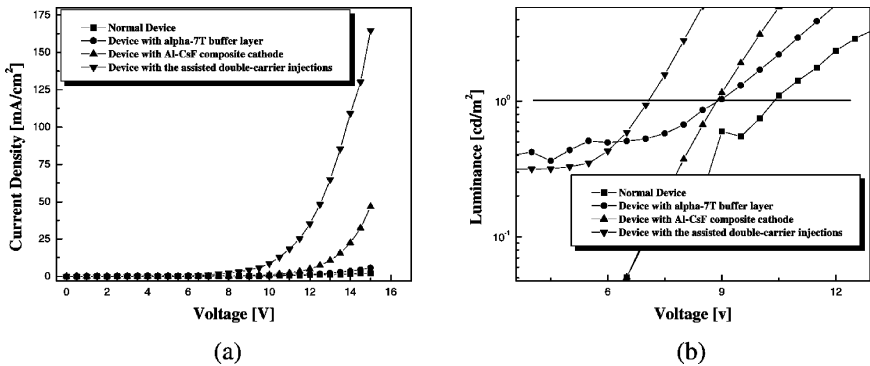


**FIGURE 7** (a)  $J$ - $V$  characteristics and (b)  $L$ - $V$  characteristics of the fabricated devices.



**TABLE 1** Turn-on Voltages and Luminance Characteristics of the Fabricated Devices

Device	Turn-on voltage	Luminance at 4 mA/cm <sup>2</sup>
Normal device	10 V	95 cd/m <sup>2</sup>
Device with $\alpha$ -7T buffer layer	9 V	110 cd/m <sup>2</sup>
Device with composite cathode	9 V	160 cd/m <sup>2</sup>
Device with $\alpha$ -7T buffer layer and composite cathode	7 V	172 cd/m <sup>2</sup>

assisted double-carrier injections shows the largest current density at the same voltage and the lowest turn-on voltage, 7 V. The turn-on voltages, which are defined as a voltage at 1 cd/m<sup>2</sup> in this experiment, are summarized in Table 1. Device by assisted double-carrier injections also shows the highest luminance, for example 172 cd/m<sup>2</sup> at 4 mA/cm<sup>2</sup>, compared with the other devices. Luminance characteristics at 4 mA/cm<sup>2</sup> are also detailed in Table 1. These results are due to the improved carrier injections from both electrodes and the balanced carrier densities by assisted double-carrier injections.

## SUMMARY

We fabricated devices with  $\alpha$ -7T buffer layer and Al-CsF composite cathode. Upon the investigations, the horizontally oriented  $\alpha$ -7 with 20 nm and the composite cathode composed of Al-CsF (3 wt%) are the optimized conditions for hole and electron injections, respectively. In the device with this structure, the assisted double-carrier injections could be obtained by lowering the energy barriers for carrier injections at electrode/organic interfaces. Device with this structure shows the lowest turn-on voltage, 7 V and the highest luminance characteristics, 172 cd/m<sup>2</sup> at 4 mA/cm<sup>2</sup>. In consequence, it can be concluded that the assisted double-carrier injections is efficient way for improving the performances of OLEDs.

## REFERENCES

- [1] Tang, C. W. & VanSlyke, S. (1987). *Appl. Phys. Lett.*, **51**, 913.
- [2] Hosokawa, C., Higashi, H., Nakamura, H., & Kusumoto, T. (1995). *Appl. Phys. Lett.*, **67**, 25.
- [3] Shimada, T., Hamaguchi, K., & Koma, A. (1998). *Appl. Phys. Lett.*, **72**, 15.
- [4] Parthasarathy, G., Burrows, P. E., Khalfin, V., Kozlov, G. G., & Forrest, S. R. (1998). *Appl. Phys. Lett.*, **72**, 17.
- [5] Shin, D. M., Lim, S. T., Choi, J. S., & Kim, J. S. (2000). *Thin Solid Films*, **363**, 268.
- [6] Pommerehne, J., Vestweber, H., Tak, Y. H., & Bassler, H. (1996). *Synth. Met.*, **76**, 67.

- [7] Videlot, C. & Fichou, D. (1999). *Synth. Met.*, **102**, 885.
- [8] Park, J. H., Lee, Y. S., Kwak, Y. H., Choi, J. S., Lim, S. T., & Shin, D. M. *J. Korean Phys. Soc.*, in press.
- [9] Yanagi, H., & Okamoto, S. (1997). *Appl. Phys. Lett.*, **71**, 2563.
- [10] Park, J. H., Lee, Y. S., Kwak, Y. H., & Choi, J. S. (2001). *KIEE International Transactions on EA 11C-3*, 43.
- [11] Parthasarathy, G., Shen, C., Kahn, A., & Forrest, S. R. (2001). *J. Appl. Phys.*, **89**, 4986.
- [12] Greczynski, G., Salaneck, W. R., & Fahlman, M. (2001). *Appl. Surface Science*, 175–176, 319.